DESY 06-065
9th May 2007

arXiv:0705.1259v1 [hep-ph] 9 May 2007

Towards a measurement of the two-photon decay width of the Higgs boson at a Photon Collider

K. Mönig[1] **and A. Rosca**[2]

[1] DESY, Zeuthen, D 15738, Germany
[2] West University of Timisoara, Timisoara, RO 300223, Roumania

Abstract

A study of the measurement of the two photon decay width times the branching ratio of a Higgs boson with the mass of 120 GeV in photon - photon collisions is presented, assuming a $\gamma\gamma$ integrated luminosity of 80 fb^{-1} in the high energy part of the spectrum. The analysis is based on the reconstruction of the Higgs events produced in the $\gamma\gamma \to$ H process, followed by the decay of the Higgs into a $\mathrm{b\bar{b}}$ pair. A statistical error of the measurement of the two-photon width,$\Gamma(H \to \gamma\gamma)$, times the branching ratio of the Higgs boson, $\mathrm{BR}(H \to \mathrm{b\bar{b}})$ is found to be 2.1 % for one year of data taking.

1 Introduction

The central challenge for particle physics nowadays is the origin of mass. In the Standard Model the masses of both fermions and gauge boson are generated through interactions with the same scalar particle, the Higgs boson H. While it can only be produced in association with another particle at an e^+e^- collider, the Higgs boson can be produced singly in the s-channel of the colliding photons at a Photon Collider. If it exists, the Higgs boson will certainly be discovered by the time such a facility will be constructed. The aim of this machine will be then a precise measurement of the Higgs properties. This facility as an upgrade option at the ILC [1] will permit a high precision measurement of the $H \to \gamma\gamma$ partial width, which is a quantity sensitive to the existence of new charged particles. For this reason such a measurement is significantly important. If we find a deviation of the two photon width from the Standard Model prediction it means that an additional contribution from unknown particles is present, and so it is a signature of physics beyond the Standard Model. For example, the minimal extension of the Standard Model predicts the ratio of the two photon width $\Gamma(H \to \gamma\gamma, \mathrm{MSSM})/\Gamma(H \to \gamma\gamma, \mathrm{SM}) < 1.2$ [2] for a Higgs boson with a mass of 120 GeV, assuming a supersymmetry scale of 1 TeV and the chargino mass parameters M and μ of 300 and 100 GeV, respectively.

At a Photon Collider one can measure the product $\Gamma(H \to \gamma\gamma)\times BR(H \to X)$. To obtain the two-photon partial width independent of the branching ratio one has to combine the above measurement with an accurate measurement of the $BR(H \to X)$ from another machine.

This study investigates the capability of an ILC detector to measure the two photon decay width times the branching ratio for a Higgs boson with the mass of 120 GeV, the preferred mass region by recent electroweak data [3]. The simulation of the signal and background processes is described in section 2. Event selection is described in section 3. Results are summarised in section 4.

The feasibility of the measurement of the two photon decay width of the Higgs boson in this mass region has also been reported by [4-6]. Our analysis presents for the first time a realistic simulation of the background processes, particularly the emission of a hard gluon.

2 Simulation of the signal and background processes

The cross section for the Higgs boson formation is given by a Breit-Wigner approximation

$$\sigma_{\gamma\gamma\to H} = 8\pi \frac{\Gamma(H \to \gamma\gamma)\Gamma_{\mathrm{tot}}}{(s_{\gamma\gamma} - M_H^2)^2 + M_H^2\Gamma_{\mathrm{tot}}^2}(1 + \lambda_1\lambda_2),$$

where M_{H} is the Higgs boson mass, $\Gamma(\mathrm{H} \to \gamma\gamma)$ and Γ_{tot} are the two photon and total decay width of the Higgs boson, λ_1 and λ_2 are the initial photon helicities and $\sqrt{s}_{\gamma\gamma}$ is the $\gamma\gamma$ centre-of-mass energy. The initial photons should have equal helicities, so that $J_{\mathrm{z}} = 0$, in order to make a spin-0 resonance as it is the case of the Higgs boson. If polarised photon beams are used, the signal cross section is increased up to a factor of 2. The experimentally observed cross section is obtained by folding this basic cross section with the $\gamma\gamma$ collider luminosity distribution.

A Higgs boson with standard model coupling and a mass of 120 GeV can be produced in the $\gamma\gamma \to \mathrm{H}$ process. In this mass region the Higgs particle will decay dominantly into a $\mathrm{b\bar{b}}$ pair. The event rate is given by the formula:

$$N(\gamma\gamma \to \mathrm{H} \to \mathrm{b\bar{b}}) = \frac{\mathrm{d}\mathcal{L}_{\gamma\gamma}}{\mathrm{d}\sqrt{\mathrm{s}}_{\gamma\gamma}}|_{\mathrm{M_H}} \frac{4\pi^2 \Gamma(\mathrm{H} \to \gamma\gamma)\mathrm{BR}(\mathrm{H} \to \mathrm{b\bar{b}})}{\mathrm{M_H^2}}(1 + \lambda_1\lambda_2)(\hbar\mathrm{c})^2,$$

where the conversion factor $(\hbar c)^2$ is $3.8937966{\cdot}10^{11}$ fb GeV^2. This rate depends strongly on the value of the differential luminosity at the Higgs mass, $\frac{d\mathcal{L}_{\gamma\gamma}}{\mathrm{d}\sqrt{\mathrm{s}}_{\gamma\gamma}}|_{M_{\mathrm{H}}}$.

High energy photon beams can be produced at a high rate in Compton backscattering of laser photons off high energy electrons [7]. The beam spectra at $\sqrt{s}_{ee} = 210$ GeV are simulated using the CompAZ [8], a fast parameterisation which includes multiple interactions and non-linearity effects. The shape of the luminosity distribution depends on the electron and laser beam parameters. The electron and laser beam energy considered for this study are 105 GeV and 1 eV, respectively, resulting in the maximum photon energy of about 70 GeV, suitable to study a Higgs boson with the mass of 120 GeV. Setting opposite helicities for the laser photons and the beam electrons the energy spectrum of the backscattered photons is peaked at about 60% of the e^- beam energy. The number of high energy scattered photon is nearly two times higher if we use polarised photons and electrons with opposite helicities than in the case of unpolarised electron and laser photons. Consequently, this leads to an improved luminosity in the high energy part of the spectrum. The scattered photons are highly polarised in this high energy region. The helicity combination of the two high energy photons can be arranged such that $J_{\mathrm{z}} = 0$ state is dominant. The resulting value of $\frac{d\mathcal{L}_{\gamma\gamma}}{\mathrm{d}\sqrt{\mathrm{s}}_{\gamma\gamma}}|_{M_{\mathrm{H}}}$ is 1.6 fb^{-1}/GeV in one year of running using the parameters from [7].

The branching ratios $\mathrm{BR}(\mathrm{H} \to \gamma\gamma)$, $\mathrm{BR}(\mathrm{H} \to \mathrm{b\bar{b}})$ and the total width are taken to be 0.22%, 68% and 4 MeV, respectively. These numbers are calculated with HDECAY [9] program and include QCD radiative corrections. With an integrated luminosity of 80 fb^{-1} per year in the hard part of the spectrum [7] about 20000 signal events can be produced under these conditions.

The signal $\gamma\gamma \to \mathrm{H} \to \mathrm{b\bar{b}}$ process is simulated with PYTHIA [10]. A total of 100K events were generated. Parton evolution and hadronisation are simulated using the parton shower and the string fragmentation models.

The main background processes to an intermediate mass Standard Model

Higgs production are the direct continuum $\gamma\gamma \to b\bar{b}$ and $\gamma\gamma \to c\bar{c}$ production. The light quarks are very efficiently rejected by the b-tagging. Due to helicity conservation, the continuum background production proceeds mainly through states of opposite photon helicities, making the states $J_z = 2$. Choosing equal helicity photon polarisations the cross section of the continuum background is suppressed by a factor $M_q^2/s_{\gamma\gamma}$, with M_q being the quark mass. Unfortunately, this suppression does not apply to the process $\gamma\gamma \to q\bar{q}g$, because after the gluon radiation the $q\bar{q}$ system is not necessarily in a $J_z = 0$ state. The resulting background is still very large compared to the signal. Therefore, a reliable prediction of the background implies to consider the NLO QCD corrections. Exact one-loop QCD corrections have been calculated in [11] for both $J_z = 0$ and $J_z = 2$ states and most recently in [12]. For $J_z = 0$ state it has been found that double logarithmic corrections are also necessary and these were calculated and resumed to all orders in the form of a non-Sudakov form factor in [13]. For the background studies the SHERPA [14] generator has been used. SHERPA is a tree level matrix element generator which uses the CKKW [15] method to merge the matrix elements for parton production with the parton shower. Using a jet algorithm, the kinematic range for n partons is partitioned into two regions, a region of jet production which is covered by the corresponding matrix elements, and a region of jet evolution which is covered by the parton shower. In the matrix element dominated region the hard kinematics is that of n partons while in the parton shower dominated region the hard kinematics is that relevant to $n-1$ partons. In both regions, the matrix elements are reweighted with a combination of Sudakov form factors entering the shower algorithm. The hard emissions in the parton shower leading to a jet are vetoed, preventing the shower to populate this region. At the end, the physical observables will exhibit a dependence on the jet resolution parameter, y_{cut}, of the next-to-next-to-leading log nature, i.e. $\alpha_s^k log^{2k-2} y_{cut}$. We generated $q\bar{q}$ and $q\bar{q}g$ events using the value for the jet resolution parameter of 0.0001 [16]. For higher y_{cut} large discontinuities around the cut value have been observed in the $2 \to 3$ jet rate distribution as a function of y_{23}. The reason of their presence is that SHERPA, being a tree level generator, cannot simulate $q\bar{q}g$ events where one quark has very low energy or the two quarks are very collinear, so such events were missing from the simulated data sample. Such three jet $q\bar{q}g$ events, with a highly energetic gluon and the other two quarks collinear, are largely produced in the $J_z = 0$ state since the M_q^2/s suppression is compensated by an α_s/s factor in the cross section. Finally, the total cross sections given by SHERPA for the $b\bar{b}(g)$ and $c\bar{c}(g)$ processes for the $J_z = 0$ state were scaled by a factor of 1.34 and 1.92 respectively, as one can see in Figure 1. These K-factors resulted from a comparison between the SHERPA cross sections and the theoretical NLO calculations.

A total of 1000K events were generated for each background process and each $\gamma\gamma$ spin state.

A convolution with the luminosity distribution is performed and a kinematic

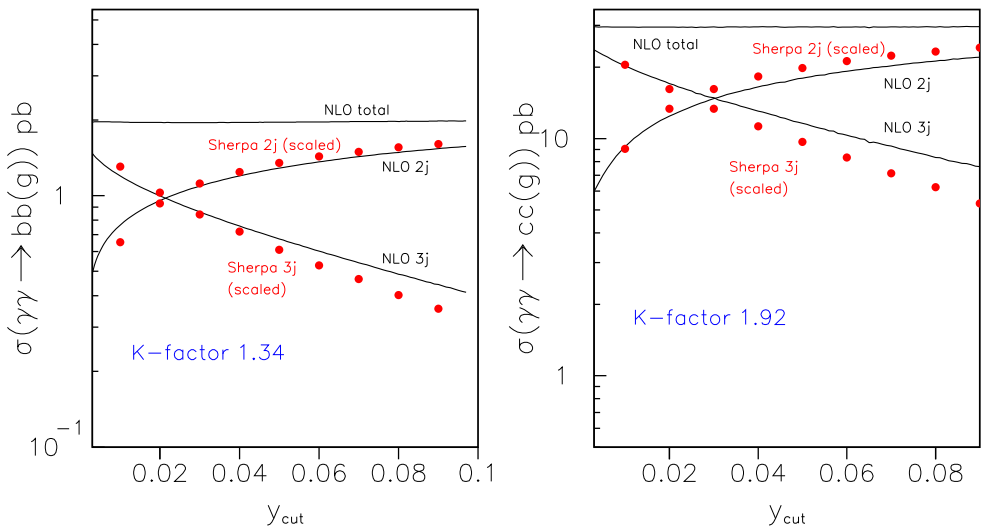

Figure 1: Scaled SHERPA cross sections for $J_z = 0$ compared to the NLO calculations for a) $\gamma\gamma \to b\bar{b}(g)$ and b) $\gamma\gamma \to c\bar{c}(g)$.

cut of $\sqrt{s}_{\gamma\gamma}$ greater than 80 GeV is imposed during the event generation for both signal and background processes.

The response of the detector has been simulated with SIMDET 4 [17], a parametric Monte Carlo for the TESLA e^+e^- detector. It includes a tracking and calorimeter simulation and a reconstruction of energy-flow-objects (EFO). Only EFOs with a polar angle above 7^0 can be taken for the Higgs reconstruction simulating the acceptance of the photon collider detector as the only deference to the e^+e^- detector [18].

The hadronic cross-section for $\gamma\gamma \to$hadrons events, within the energy range above 2 GeV, is several hundred nb [19], so that about 1.0 event of this type is produced per bunch crossing. These events (pile-up) are overlayed to the signal events. Since the pile-up events are produced in the t-channel q-exchange most of the resulting final state particles are distributed at low angles.

3 Event selection

An intermediate mass Higgs production leads mainly to the final state: $\gamma\gamma \to H \to b\bar{b}$. The major characteristics of these events, used to distinguish the signal from the background, are the event topology and the richness in b quarks. The background consists of multi-jet events coming from $\gamma\gamma \to q\bar{q}(q)$ processes.

In order to minimise the pile-up contribution to the high energy signal tracks the first step in the separation procedure was to reject pile-up tracks as much as possible. The measurement of the impact parameter of a particle along the beam axis with respect to the primary vertex is used for this purpose, as described in

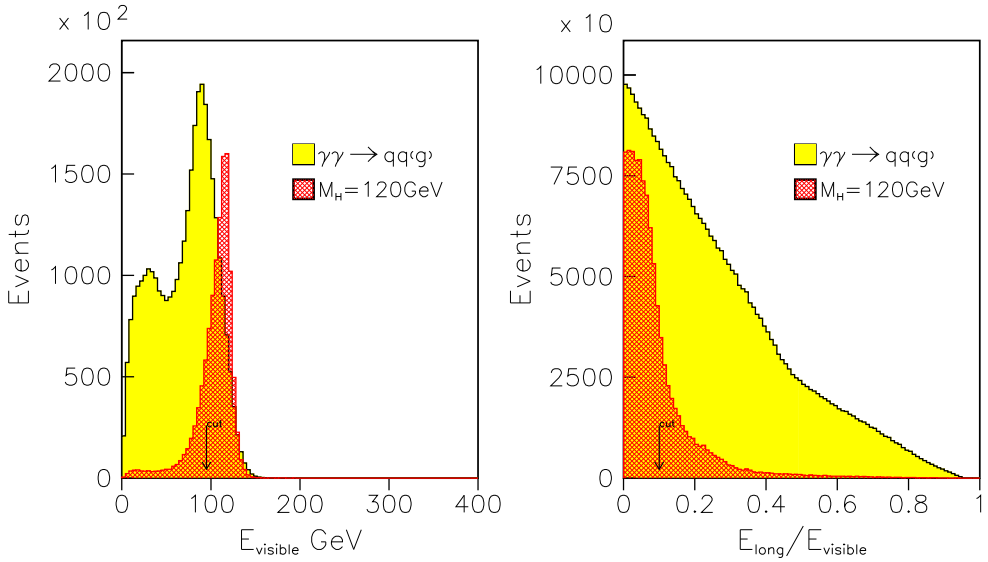

Figure 2: Left: Distributions of the visible energy and Right: of the longitudinal imbalance for signal (M_H = 120 GeV) and background. The distribution for the signal is arbitrarily normalised. Events with pile-up.

Ref. [20]. A reconstruction of the angle of each EFO with respect to the z-axis, θ_{EFO} makes it possible to distinguish further between signal and pile-up EFOs. EFOs are rejected if $|\cos(\theta_{EFO})|$ >0.950.

Hadronic balanced events are then selected requiring: large particle multiplicity (at least 5 EFO), large visible energy ($E_{visible}$ greater than 95 GeV) and small longitudinal imbalance, normalised to the visible energy (not larger than 0.1). Figure 2 shows the distributions of the visible energy and the longitudinal imbalance.

Due to the fact that the Higgs is centrally produced, the requirement that the thrust of the event, see Figure 3 left , points in the central region of the detector ($|\cos\theta_{thrust}| \leq 0.7$) allows to reduce further the background while keeping a large fraction of the signal.

In the remaining event sample jets are reconstructed using the DURHAM clustering scheme [21] with the resolution parameter $y_{cut} = 0.02$. Events are kept only if there are at least 2 such jets.

The cross section for the continuum production of the charm quark is 16 times larger than for bottom quarks. Therefore one of the most critical issues for this analysis is the capability of the detector to identify events in which a b quark is produced. To this aim a b-tagging algorithm based on a Neural Network has been applied. The algorithm combines several discriminating variables, as for example, the impact parameter joint probability introduced by ALEPH [22] and the p_t corrected vertex invariant mass obtained with the ZVTOP algorithm written for the SLD experiment [23] into a feed forward Neural Network with 12

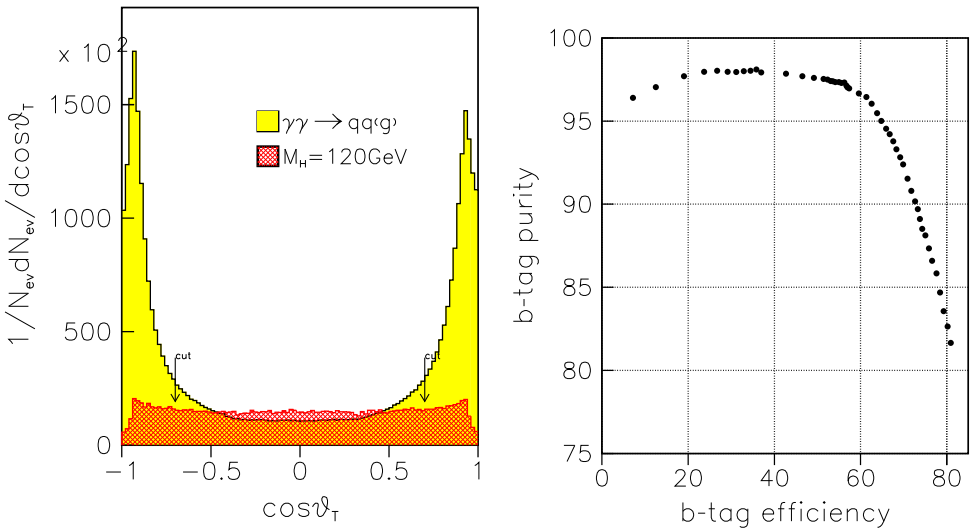

Figure 3: Left: Distribution of the absolute value of the cosine of the thrust angle for signal (M_H = 120 GeV) and background. The distribution for signal is arbitrarily normalised. Events with pile-up. Right: Efficiency on b quarks and b-purity of the b-tagging for simulated $q\bar{q}$ events at $\sqrt{s} = M_Z$.

inputs and 3 output nodes, described in Ref. [24].

Figure 3 right shows the efficiency on b-quarks and the b-quark purity for the algorithm exploited. It has been obtained on a Monte Carlo sample of $q\bar{q}$ events at $\sqrt{s} = M_Z$. The b-tagging efficiency corresponding to a purity of 97% is 50%.

The b-quarks coming from the decay of the Higgs boson are highly energetic, whereas in the case of the background processes the gluon and one b-quark jet are the most energetic. This is shown for 3-jet events in Figure 4. In order to reduce the background further we look at the two fastest jets in the event and require the $\mathrm{NN_{out}}$ to be greater than 0.9 for one jet and greater than 0.1 for the second one. This procedure is also efficient for 2-jet events. There is a large number of 2-jet background events where one b is low energetic or both b-quarks are collinear so that they get merged into one jet. For this reason 40% of the J=0 2-jet events are rejected by the b-tagging cut on the second jet while only 15% of the signal events fail this cut.

The total signal efficiency is estimated to be 22% in the presence of the pile-up events.

4 Results

The reconstructed invariant mass for the selected signal and background events is shown in Figure 5. Here the invariant mass is corrected for escaping neutrinos as in Ref. [5]. To enhance the signal a cut on the invariant mass is tuned such that

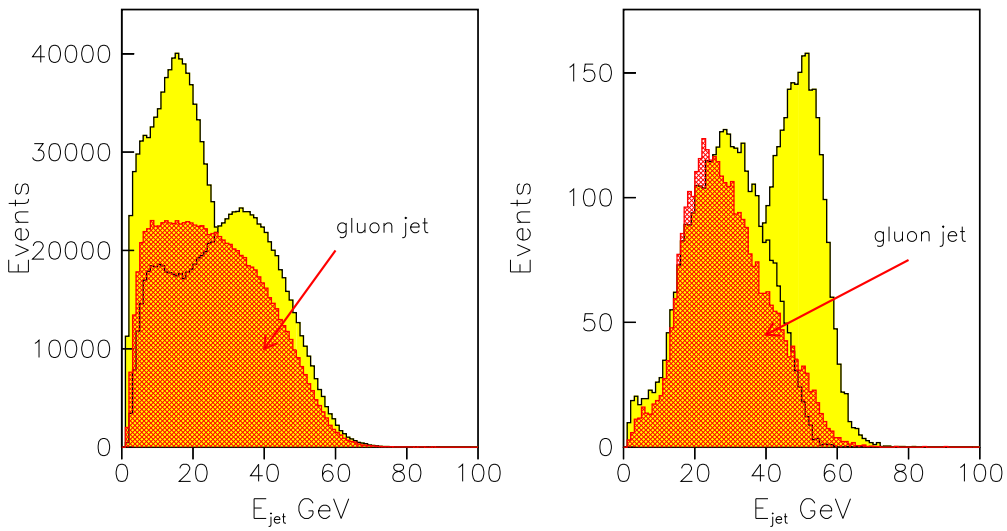

Figure 4: Distributions of the b-quarks and gluon jets for the background (left) and the signal (right). Events with pile-up.

the statistical significance of the signal over background is maximised. Events in the mass region of 112 GeV $< M_{jets} <$ 134 GeV are selected. The number of estimated signal and background events in this window are 3534 and 2170, respectively.

The two photon decay width of the Higgs boson is proportional to the event rates of the Higgs signal. The statistical error of the number of signal events, $\sqrt{N}_{\rm obs}/(N_{\rm obs} - N_{\rm bkg})$, corresponds to the statistical error of this measurement. Here $N_{\rm obs}$ is the number of observed events, while $N_{\rm bkg}$ is the number of expected background events.

We obtain

$$\frac{\Delta[\Gamma(\mathrm{H} \to \gamma\gamma) \times \mathrm{BR}(\mathrm{H} \to \mathrm{b\bar{b}})]}{[\Gamma(\mathrm{H} \to \gamma\gamma) \times \mathrm{BR}(\mathrm{H} \to \mathrm{b\bar{b}})]} = \sqrt{N}_{\rm obs}/(N_{\rm obs} - N_{\rm bkg}) = 2.1\%.$$

5 Conclusions

The photon collider option at the ILC offers the possibility to measure the partial width of the Higgs into photons, $\Gamma(\mathrm{H} \to \gamma\gamma)$. Taking higher order QCD corrections for the background into account and using realistic assumptions for the detector and background from pileup events We conclude that for a Higgs boson with a mass $M_{\rm H} = 120$ GeV $\Gamma(\mathrm{H} \to \gamma\gamma) \times \mathrm{BR}(\mathrm{H} \to \mathrm{b\bar{b}})$ can be measured to 2.1%. Using $\Delta\mathrm{BR}(\mathrm{H} \to \mathrm{b\bar{b}}) = 2$ - 3% from the e^+e^- mode of the ILC [25] the photonic width of the Higgs can be determined to 3%. At this accuracy one can distinguish between the Standard Model Higgs particle and the lightest scalar Higgs boson predicted by models beyond the Standard Model. Also, the precise

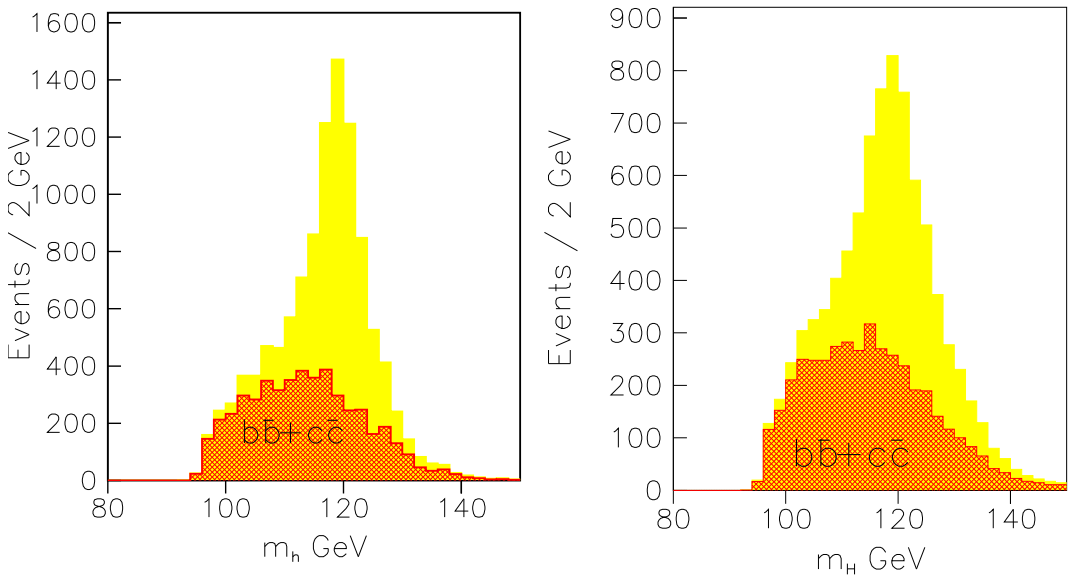

Figure 5: Higgs invariant mass reconstruction on signal and background for a Higgs mass of 120 GeV without (left) and with (right) pile-up events overlayed.

measurement of the decay width $\Gamma(\mathrm{H} \to \gamma\gamma)$ can reveal heavy charged particles circulating in the loop, as for example supersymmetric particles. The accuracy of the mass determination of the heavier stop $\tilde{t}_2$ is estimated to be 10 - 20 GeV in [26], assuming that the lighter stop $\tilde{t}_1$ and the mixing angle $\theta_{\tilde{t}}$ are known.

References

[1] Parameters for the Linear Collider
`http://www.fnal.gov/directorate/icfa/LC_parameters.pdf`.

[2] D.L. Borden, D.A. Bauer and D.O. Caldwell, Phys. Rev. D48 (1993) 4018.

[3] The ALEPH, DELPHI, L3, OPAL Collaborations and the LEP Electroweak Working Group, A combination of Preliminary Electroweak Measurements and Constraints on the Standard Model, CERN-PH-EP/2006-042, hep-ex/0612034.

[4] T. Ohgaki, T. Takahashi and I. Watanabe, hep-ph/9703301; G. Jikia and S. Söldner-Rembold, Nucl. Instr. and Meth. A472 (2001) 133.

[5] P. Niezurawski, A.F. Zarnecki and M. Krawczyk, Acta Phys. Polon. B34 (2003) 177.

[6] P. Niezurawski, Ph.D. thesis, hep-ph/0503295

[7] B. Badelek *et al.*, *TESLA Technical Design Report Part VI, Chapter I: The Photon Collider at TESLA*, DESY-01-011.

[8] A.F. Zarnecki, Acta Phys. Polon. B34 (2003) 2741.

[9] A. Djouadi, J. Kalinowski and M. Spira, Comp. Phys. Comm. 108 (1998) 56.

[10] T. Sjöstrand, CERN-TH/7112/93 (1993), revised August 1995; T. Sjöstrand, Comp. Phys. Comm. 82 (1994) 74.

[11] G. Jikia and A. Tkabladze, Phys. Rev. D54 (1996) 2030.

[12] V.A. Khoze, M.G. Ryskin and W.J. Stirling, hep-ph/0607134.

[13] M. Melles and W.J. Stirling, Phys. Rev. D59 (1999) 94009; M. Melles and W.J. Stirling, Eur. Phys. J. C9 (1999) 101.

[14] T. Gleisberg, S. Höche, F. Krauss, A. Schälicke, S. Schumann and J. Winter, JHEP 0402 (2204) 056 (hep-ph/0311263).

[15] S. Catani, F. Krauss, R. Kuhn and B.R. Webber, JHEP 0111 (2001) 063.

[16] K. Mönig and A. Rosca, Acta Phys. Polon. B37 (2006) 1181.

[17] M. Pohl and H.J. Schreiber, SIMDET-version4, *A Parametric Monte Carlo for a TESLA Detector*, DESY-02-061.

[18] F. Bechtel *et al.*, Nucl. Instrum. Meth. A564 (2006) 243.

[19] The Particle Data Group, K. Hagiwara *et al.*, Phys. Rev. D66 (2002) 010001.

[20] K. Mönig and I. Sekaric, Eur. Phys. J. C38 (2005) 427.

[21] S. Bethke *et al.*, Nucl. Phys. B370 (1992) 310.

[22] D. Buskulic *et al.* [ALEPH Collaboration], Phys. Lett. B313 (1993) 535.

[23] D.J. Jackson, Nucl. Instr. Meth. A388 (1997) 247.

[24] R. Hawkings, LC-PHSM-2000-021.

[25] J.A. Aguilar-Saavedra *et al.*, TESLA Technical Design Report, Part III: Physics at an e^+e^- Linear Collider. DESY-01-011c, hep-ph/0106315.

[26] D. Asner *et al.*, hep-ph/0208219.

Acknowledgments

The authors would like to thank Georgi Jikia, Frank Krauss and Andreas Schälicke for many interesting discussions. Part of this work was supported by the CEEX Program of the Romanian Ministry of Education, Research and Youth, contract 05-D11-81/21.10.2005.